Deltares

Borssele II: Site evaluation

Hydro and meteo hazards

Borssele II: Site evaluation
Hydro and meteo hazards

Client	Ministerie van Economische Zaken en Klimaat
Contact	
Reference	-
Keywords	-

Document control	
Version	1.0
Date	17-01-2024
Project nr.	11209639-005
Document ID	11209639-005-GEO-0002
Pages	42
Classification	Confidential until further notice
Status	Final

Summary

This document provides an overview of the various hydro- and meteohazards that can occur in the vicinity of the proposed site of the Borssele 2 powerplant. The data presented in the document are based on previous studies, literature, existing data and expert judgement. In addition to giving an overview of the existing knowledge and understanding of the potential hazards, this document also aims at providing an overview of the available sources of information. As such, this document can form the basis for a detailed and comprehensive evaluation of hydro- and meteohazards if required during the latter stages of development.

Contents

1 Introduction

1.1 Background

The Ministry of Economic Affairs and Climate Policy of the Netherlands requested Deltares to conduct a subsurface site evaluation for the intended Borssele II nuclear power plant site in the Zeeland province of the Netherlands. Within the scope of these studies are the external hazards as described in chapter 5 of IAEA-SSR-1:

- Evaluation of extreme meteorological hazards.
- Evaluation of rare meteorological events.
- Evaluation of flooding hazards.
- Changes of hazards and site characteristics with time.

This document provides a hazard assessment regarding potential meteorological and hydrological hazards facing the potential Borssele site[1]. The various aspects of the site survey will focus on the hazard assessment and the data required to perform a reliable assessment of hazards. As the design of the Borssele 2 facility or the location of the facility is yet unknown, the site survey did not include an assessment of the vulnerability or risk of damage or failure of the facility in relation to the identified hazards.

1.2 Objective

The objective of the site survey is to make an inventory of all relevant meteorological and hydrodynamic hazards that can occur at Borssele 2 location based on a literature study as well as expert judgements.

In addition to the assessment of the hydrological and meteorological hazards at the Borssele site, an initial screening of the extreme statistics of wind speed, waves, and water levels (high and low) in the direct vicinity of the plant was assessed as this was considered relevant as input for following design stages.

The type of hydrological and meteorological hazards that were addressed was based on the Specific Safety Guide regarding these hazards, set up by the International Atomic Energy Agency (IAEA, 2011). This document will address the variables:

- Wind speed (article 2.7 in IAEA (2011).
- Post-tropical cyclones (article 2.8).
- Extreme precipitation (article 2.7).
- Tsunamis (article 2.11).
- Seiches (article 2.11).
- Extreme water levels (article 2.11).
- Temperature (article 2.6)

1.3 Setup of the report

In chapter 2, an overview of the different hazards is presented based on literature and existing data. This is followed by concluding remarks and recommendations. Detailed literature and data reviews for the various hazards are presented in the appendices.

[1] This document does not address potential hazards regarding other potential sites.

2 Hazards assessment

2.1 Extreme wind conditions

In the Netherlands wind speed has been measured for decades at various stations near the coast and inland. Near Borssele a station is available in Vlissingen, where the wind speed is measured for more than 40 years. For this station the extreme statistics have been defined based on the annual maxima of the so-called potential wind speed.

For the safety assessment and design of dunes and dikes along the Dutch coast, a probabilistic tool is used to determine hydraulic loads, called Hydra-NL. Based on the directional extreme value distribution for the wind speed at Vlissingen, a non-directional wind speed exceedance chart has been constructed (see Appendix A for further details), visually shown in Figure *2.1*. The probability of exceedance chart indicates that approximately once every 4 to 5 thousand years an hourly wind speed of 36 m/s (Beaufort 12) is exceeded at Vlissingen.

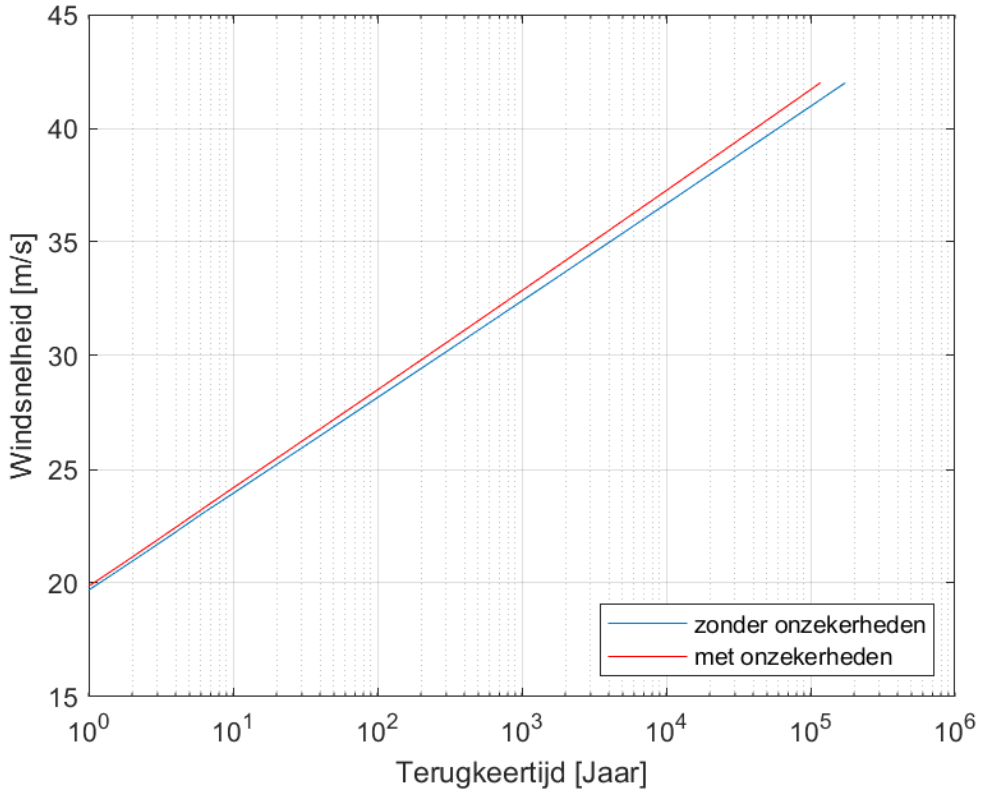

Figure 2.1 Probability of exceedance for the hourly wind speed at Vlissingen; blue line is without statistical uncertainties (x-axis: Return period [year]; y-axis: wind speed [m/s]). See Appendix A for details.

2.2 Extra tropical cyclones

Appendix B provides the literature review carried out by the KNMI. Here the main findings are presented.

Tropical cyclones, or hurricanes, are extremely powerful storms that can develop over areas with warm sea water. Some tropical cyclones develop off the African West Coast and move northward along the US East Coast, losing their tropical character and turning into an extra-tropical storm. At the height of Newfoundland these post-tropical cyclones are carried by the jet stream towards Europe, and on the way they can regain strength under favourable conditions. A warming climate might contribute to increased frequency and intensity of post-tropical cyclones in Europe.

A study on European cyclones with tropical origin in reanalysis data revealed that in the period 1979-2013 53 hurricanes have entered the European area. A very few of them still had hurricane strength when they hit the western part of the British Isles. The Netherlands has never been hit by a post-tropical cyclone with hurricane force (Beaufort 12; > 36 m/s). From the observational data the conclusion is therefore that the risk of the Netherlands being hit by a post-tropical cyclone with Beaufort 12 is negligible.

In 2017 Europe was hit by hurricane Ophelia, which due to high water temperatures regained strength prior to passing the Irish coastline. Ophelia can be considered as a showcase for cyclone characteristics in a warmer climate. The British Isles are not necessarily the only area exposed to off-track tropical cyclones: according to a model simulation, Ophelia could just as well have squeezed through the Straits of Calais to reach the Dutch coast with hurricane force winds. Further climate studies confirmed the increased risk of Western Europe to be hit by extra-tropical storm that origin from hurricanes. Further research is however required to quantify this risk further.

2.3 Extreme precipitation with the potential to induce local flooding

Appendix B provides the literature review carried out by the KNMI. Here the main findings are presented.

For the proposed location of the Borssele 2 powerplant a literature study is carried out regarding the precipitation risk, as extreme precipitation (both intensity and duration) may lead to local flooding.

Frequency statistics of (extreme) rain in the Netherlands is provided by STOWA (2019) as the amount of rain for a given rainfall duration (two hours to eight days), which is exceeded with a certain frequency (Figure 2.2). The average amount of precipitation per year in the Netherlands increased by 9% between 1961-1990 and 1991-2020. However, rainfall during extreme wet days increased by 15%. In a warmer climate, the atmosphere can contain more water vapor and, therefore, extreme showers are expected to occur more often in the future. In the KNMI'14 climate scenarios precipitation extremes increase throughout the year, even in the scenarios with an overall drying in summer. In summer the daily amount exceeded once in 10 years increases by 2-22% around 2050 and 3-40% around 2085. The maximum hourly amount per year increases by 6-25% around 2050 and 8-45% by 2085. In October 2023 the KNMI'23 climate scenarios will be published. First results indicate that the increase in moderate extreme hourly precipitation will be smaller and the increase in the highest extremes (above 50 mm per hour) will be about similar to the KNMI'14-scenarios.

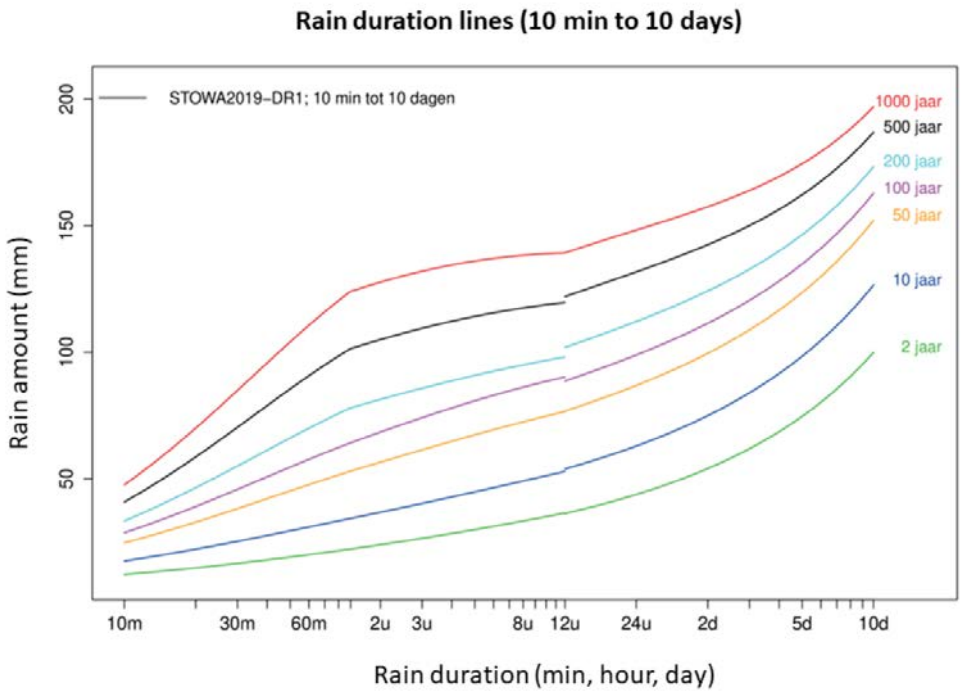

Figure 2.2 Rain duration lines based on precipitation observations in the Netherlands for the whole year. Source: STOWA (2019).

2.4 Tsunamis

Tsunamis are waves propagating in the sea because of a sudden vertical displacement of the water column. Offshore, tsunamis can have wavelengths of up to a few 100 km's and wave amplitudes of usually less than 1 m. When tsunami waves approach the coast, the propagation speed decreases and the amplitude increases, potentially leading to coastal inundation.
Potential sources of tsunamis reaching the Dutch coast may be from subsea earthquakes at (distant) subduction zones or at (local) fault zones, subsea landslides, erupting or collapsing volcanoes, meteorites, or fast-propagating storm fronts along the coast (meteo-tsunamis).

The literature study (see Appendix C) on tsunamis potentially affecting the Dutch coast showed that the chance of a destructive tsunami reaching the Dutch coast is considered to be very low, because the North Sea is not in a tsunami-prone region and because tsunamis that do propagate from remote areas will largely dissipate due to the shallow waters of the southern part of the North Sea. Tsunamis affecting the Dutch coastline are either formed because of a landslide in the northern part of the North Sea or a local earthquake-generated tsunami in the southern part of the North Sea. Either can result in maximum wave heights of between 1.5m to 2m. However, the probability of occurrence of these events is very low (about once in 100.000 years). Other tsunamigenic sources, such as from earthquakes at remote subduction zones, volcanoes or meteorites, are not expected to result in significant tsunami wave heights at the Dutch coast. Most probable cause of tsunami wave heights of up to 1m are from fast moving storm fronts (meteotsunamis or seiches, see also Section 2.5). It is expected that tsunami wave heights will be lower at the Borssele site compared to the values reported for the Dutch coast, due to dissipation. However, no quantified data or information is yet available to confirm this.

2.5 Seiches

Seiches are standing, resonant long waves inside (semi-)enclosed basins. The Western Scheldt is considered as one of the areas where seiches can appear. Seiches in the Western Scheldt are typically caused by weather processes. Seiches can cause safety and operational issues for example at harbours, and they can add to the hydraulic loading on coastal structures and developments. Seiches in (semi-)enclosed basins along the Dutch coast are generally generated as a result of the long waves generated by the squall-induced pulses and oscillations at the open sea.

For the Borssele 2 site, long waves generated are solely considered without local effect of resonance (the seiche) that can occur in (semi-)enclosed basins, as it is unknown for now whether a local geometry will play a role in potential local resonant responses.

Based on literature review, the best estimate currently available of a representative long wave amplitude incoming from the North Sea and that can potentially induce seiches at Borssele site is 0.30m (see Appendix D). The long-wave events on the North Sea, and the resulting seiche events inside the ports along the Dutch coast, are generated by passing low-pressure systems and cold fronts. All events coincide with a storm, although not all storms lead to seiche events. In absence of a port or other semi-confined geometry, a local seiche is not triggered and the incoming long wave from the North Sea passes the area un-amplified. Due to dissipation the amplitude will become lower as the long waves propagate further into the Western Scheldt

2.6 Water levels

For extreme water levels, various conditions can be considered, as the extreme water levels are formed by a combination of various contributing factors. Included in this hazard assessment are the return period of extreme water levels due to storms and tides, sea level rise and extreme wave heights. These aspects are assessed separately (Appendix A).

Please note that other aspects are not included in this preliminary hazard assessment, for example (but not exclusively):

- Effect of climate change on storms, and subsequently surge in water levels is not included. KNMI'14 scenarios suggest a change in the daily averaged maximum windspeed per year of between -2% and +2% for 2085, depending on the climate scenario (KNMI, 2015).
- Future changes in the tidal propagation through the estuary. Although tides itself are extremely predictable, the local propagation of the tidal wave is dependent on the local conditions. Changes in the tide can arise for instance due to morphologic changes in the bathymetry or lay-out of the estuary. This can occur either by natural processes or due to dredging and/or dumping of sediment. For example, the tidal amplitude in the Scheldt estuary has significantly changed over the last century (Taal et al., 2015).

For the safety assessment and design of dunes and dikes use is made of a probabilistic tool to determine hydraulic loads. These hydraulic loads in terms of local water levels and wave conditions can be determined for arbitrary probabilities of exceedance.

2.6.1 Extreme water level

At Vlissingen water levels are being measured since 1881. This historical dataset has been used to determine the extreme value distribution of the water level. These distributions have been corrected for the effect of sea level rise until now. Like the presentation of wind speed, the omnidirectional distribution has been determined and presented in Figure 2.3, both without (blue line) and with red line) statistical uncertainty. The 1/10.000-year value is 5.5m + NAP.

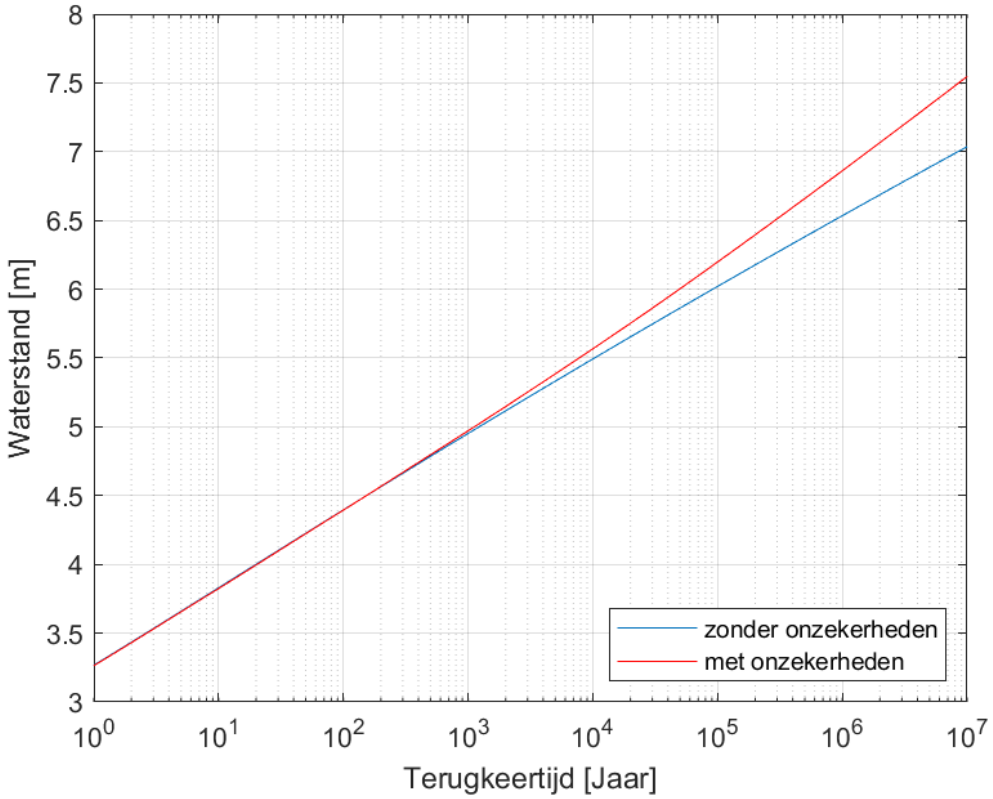

Figure 2.3 Probability of exceedance curve of the water level at Vlissingen, with and without the statistical uncertainty integrated (x-axis: Return period [year]; y-axis: water level [m NAP]).

2.6.2 Sea level rise

The KNMI published in 2014 (KNMI, 2015) the projected effects of climate change for four different scenarios. The projected sea level rise for 2050 was estimated between +15cm and +40cm, whereas sea level rise was expected to accelerate in the later stages of the century resulting in a sea level rise between +25cm to +80cm for 2085.

In 2021, the KNMI published preliminary results of a revision to be published later this year (KNMI, 2021). Here it is stated that the expected sea level rise for 2100 is up to 1.2m . This bandwidth is significant (ranging from 0.3m to 1.2m SLR) and for a large part determined by the uncertainty in the rate of mass-loss of the Antarctic ice sheet[2].

In October 2023 the KNMI'23 climate scenario's will be published. Although preliminary conclusions can already be drawn, it is recommended that the site evaluation of expected water levels (among other parameters) is evaluated again against these additional data.

[2] The estimate has probability of 90% and includes the effect of land subsidence (KNMI, 2021). However, the KNMI'23 scenarios can diverge from these values.

2.6.3 Extreme wave height

As presented in Appendix 4A the extreme value distribution for wave height is very dependent on the bed level on the seaward side of the study-location. Wave breaking at the foreshore increases with more shallow water depths and can reduce the wave height at the coastal defenses surrounding the proposed site. The 1/10.000-year wave height exceedance value varies from 1.5m to 3.3m. Further details regarding the layout of the powerplant (primarily its location and surrounding bed levels towards the Western Scheldt) can help reduce this uncertainty.

2.7 Temperature, Drought & heatwaves

The maximum and minimum air temperatures are computed from the KNMI daily observation archive available at https://daggegevens.knmi.nl/ . This archive is also used to compute the highest and lowest values for the long-term (10 and 30 days) and short-term (1, 2 and 5 days) temperature averages. Also the relative humidity and sea level pressure values are computed from this archive. 100 year-return periods for maximum and minimum temperature are computed by fitting a GEV (Generalized Extreme Value) distribution to the highest annual maximum temperature and lowest annual minimum temperature, using the tool 'Trends in return times of extremes' of the KNMI Climate Explorer https://climexp.knmi.nl/.

The maximum and minimum temperatures are computed for the KNMI weather stations in Vlissingen and Westdorpe. The other parameters are computed for Vlissingen. The Vlissingen and Westdorpe records start in 1906 and 1991, respectively. See table below for a summary of indicated data.

Table 2.1 Summary of temperature related data.

Parameter	Value
Maximum and Minimum Air Temperatures	Highest maximum temperature: Vlissingen: 37.3°C (25 July 2019, measurements since 1906), Westdorpe: 40.6°C (25 July 2019, measurements since 1991) Lowest minimum temperature: Vlissingen: -18.9°C (21 Feb 1956), Westdorpe: -14.9°C (25 Jan 2013)
100 year-return period for Maximum and Minimum Air Temperature	100 year-return period and [95% range], Vlissingen, climate of 2020: Maximum temperature, 37.1 [35.4 to 38.7]°C, Minimum temperature: -16.9 [-20.7 to -13.0]°C
Long-term Base Temperature (extreme temperature for periods > 7 days)	Highest N-day average temperature, Vlissingen: N=10: 22.9°C (in 2022), N=30: 22.2°C (in 2006) Lowest N-day average temperature, Vlissingen: N=10: -8.6°C (in 1929), N=30: -4.6°C (in 1962)
Short-term Daily Temperature (extreme temperature for periods between 6 hours and 7 days)	Subdaily: not easily available, need to be separately computed from hourly data. Highest, Vlissingen, N=1: 27.9°C (in 2014), N=2: 27.0°C (in 2020), N=5: 26.3°C (in 2020) Lowest, Vlissingen: N=1: -11.8°C (in 1938), N=2: -11.4°C (in 1938), N=5: -10.3°C (in 1929)
Instantaneous Temperature (extreme temperature for a 6-hour period)	Not readily available, need to be separately computed from hourly data.
Maximum Air Humidity Conditions for the Minimum and Maximum Temperatures	Minimum relative humidity (this generally occurs about when the temperature is at the daily maximum). 25 July 2019: Vlissingen: 27%, Westdorpe: 21%. Maximum relative humidity (this generally occurs about when the temperature is at the daily minimum): Vlissingen, 21 Feb 1956: 98%, Westdorpe 25 Jan 2013: 99%.
Minimum Atmospheric Pressure	Sea level pressure: Vlissingen: 954.4 hPa (in 1985)

Maximum Atmospheric Pressure	Sea level pressure: Vlissingen: 1049.1 hPa (in 1932)

Drought in measured by KNMI by the precipitation deficit, which is approximately the sum of evaporation minus precipitation, starting the sum on 1 April, up to 30 september. The precipitation deficit has a maxium in the end of the summer. The average (1991-2020) of the maximum is 160 mm, see https://www.knmi.nl/klimaatdashboard.

Heatwaves: in De Bilt there have been 30 heatwaves since 1901, of which 14 occurred after 2000, see https://www.knmi.nl/nederland-nu/klimatologie/lijsten/hittegolven.

3 Summary and recommendations

This document provides an overview of the various hydro- and meteohazards that can occur in the vicinity of the proposed site of the Borssele 2 powerplant. The data presented in the document are based on previous studies, literature, existing data and expert judgement.

3.1 Summary

- Extreme wind conditions: The extreme value distribution of the wind speed is presented in this document, based upon measurements at Vlissingen over the period 1970 – 2008 (39 years), for example 1/10.000-year extreme wind is 37m/s.
- Extra tropical cyclones: The Netherlands has never been hit by a post-tropical cyclone with Beaufort 12 according to measurements. However, recent model studies have shown that it is possible for powerful extra tropical cyclones to hit the Netherlands, and that the probability will increase with climate change.
- Precipitation: The extreme value distribution of the precipitation presented here is based upon measurements across the Netherlands. Climate studies also provide quantified changes for precipitation for winter and summer conditions, for various time-horizons.
- Tsunamis: The chance of a destructive tsunami reaching the Dutch coast is very low and can result in maximum wave heights of between 1.5m and 2m.
- Seiches: The best estimate currently available of the long wave amplitude incoming from sea that could potentially create seiches at Borssele site is 0.30m. In absence of a (port) geometry, a resonant (seiche) response may not be triggered, and this amplitude will not be amplified.
- Water level: The extreme value distribution of the water level is presented in this document, based upon measurements at Vlissingen over a century-long period (since 1881), for example 1/10.000-year extreme water level is 5.5m + NAP. On top of that, the expected sea level rise for 2100 is potentially up to 1.2m by 2100. In addition, wave conditions strongly vary for different locations along the proposed site; the 1/10.000-year wave height exceedance value varies from 1.5m to 3.3m.

3.2 Recommendations

Two aspects are critical for a more accurate assessment of the potential meteorological and hydrodynamical hazards facing the Borssele 2 powerplant.

Firstly, the current study is based on existing data, literature and expert judgement. For a more extensive quantification of the hazards, specific studies are required:

- Numerical modelling studies to provide insights in the (hydro-)dynamics of the Western Scheldt.
- The new climate projections by the KNMI (expected later in 2023) can shed additional insight into the future conditions.
- Climate change affects various processes apart from sea level rise, such as storm surge and wave height. To be able to quantify future hazards, a more comprehensive study might be needed, combining the expected future climate change scenarios by the KNMI with detailed simulations of the hydrodynamics in the Western Scheldt.
- Once more detailed data of the site location and surrounding bed level will become available, a more comprehensive assessment of the risk due to waves can be determined.
- The extreme precipitation is now provided for a nationwide average. Local variability, for instance due to the proximity of the sea, might significantly affect these characteristics. Local data sets or numerical models might be able to highlight possible local effects.

Secondly, the various risks are at this stage assessed separately. To quantify the design criteria for the powerplant, various combinations of risks should be considered. For instance, the maximum water levels, due to tides, storms, seiches and waves should be combined to determine the design criteria for the coastal defences[3].

[3] In the current literature and data study only tides and storm surges are assessed together.

4 Literature

IAEA (2011). Meteorological and hydrological hazards in site evaluation for nuclear installations: safety guide/jointly sponsored by the International Atomic Energy Agency and the World Meteorological Organization. — Vienna.

KNMI (2015) KNMI'14-klimaatscenario's voor Nederland; Leidraad voor professionals in klimaatadaptatie, KNMI, De Bilt, 34 pp. Brochure_KNMI14_EN.pdf.

KNMI (2021) KNMI Klimaatsignaal'21: hoe het klimaat in Nederland snel verandert, KNMI, De Bilt, 72 pp. https://cdn.knmi.nl/knmi/asc/klimaatsignaal21/KNMI_Klimaatsignaal21.pdf.

Taal, M., Meerschaut, Y., Liek, G.J. (2015) Understanding The tides crucial for joint management of the scheldt Estuary. E-proceedings of the 36th IAHR World Congress 28 June – 3 July, 2015, The Hague, the Netherlands 36th IAHR World Congress. https://www.vliz.be/imisdocs/publications/273523.pdf.

Appendices

A Extreme value distributions at Borssele

By: Jacco Groeneweg
Date: June 16th, 2023

For the safety assessment and design of dunes and dikes use is made of a probabilistic tool to determine hydraulic loads. These hydraulic loads in terms of local water levels and wave conditions can be determined for arbitrary probabilities of exceedance. The basis is being formed by statistical distributions of relevant variables. For the coastal areas these are wind and water level (combination of surge and tide), and a procedure to translate combinations of stochastic values of the quantities to local water levels and wave conditions.
The probabilistic tool we use here is Hydra-NL.

A.1 Extreme wind speed

The directional extreme value distribution for the wind speed at Vlissingen, i.e. the probability of exceedance of a wind speed given a directional wind sector, is determined by Caires (2009) based upon measurements at Vlissingen over the period 1970 – 2008 (39 years). Vlissingen is close enough to Borssele to be considered as representative. From the same time series the probability of wind direction has been determined, and the result are shown in Table A-1. Clearly wind from the south-western quadrant occurs most frequent. Given the probability of occurrence of the wind direction (more specifically 12 directional sectors of 30 degrees) the omni-directional extreme value distribution for the wind speed can be determined.

The extreme value distribution of the wind speed is shown in Figure A-1. The 1/10.000 year value of the wind is 37 m/s. The figure shows two lines. In previous studies the higher (red) line is used as it includes the effects of uncertainty in the data such as noise and a limited length of a dataset.

Additionally, with the directional extreme value distribution of wind speed and the probability of occurrence of wind direction (Table A-1) a wind rose can be composed, if requested in a next stage of the hazards assessment.

Table A-1 Probability of occurrence of wind direction.

Direction	Probability	Direction	Probability
30	0.042	210	0.162
60	0.065	240	0.144
90	0.087	270	0.099
120	0.061	300	0.070
150	0.064	330	0.048
180	0.117	360	0.041

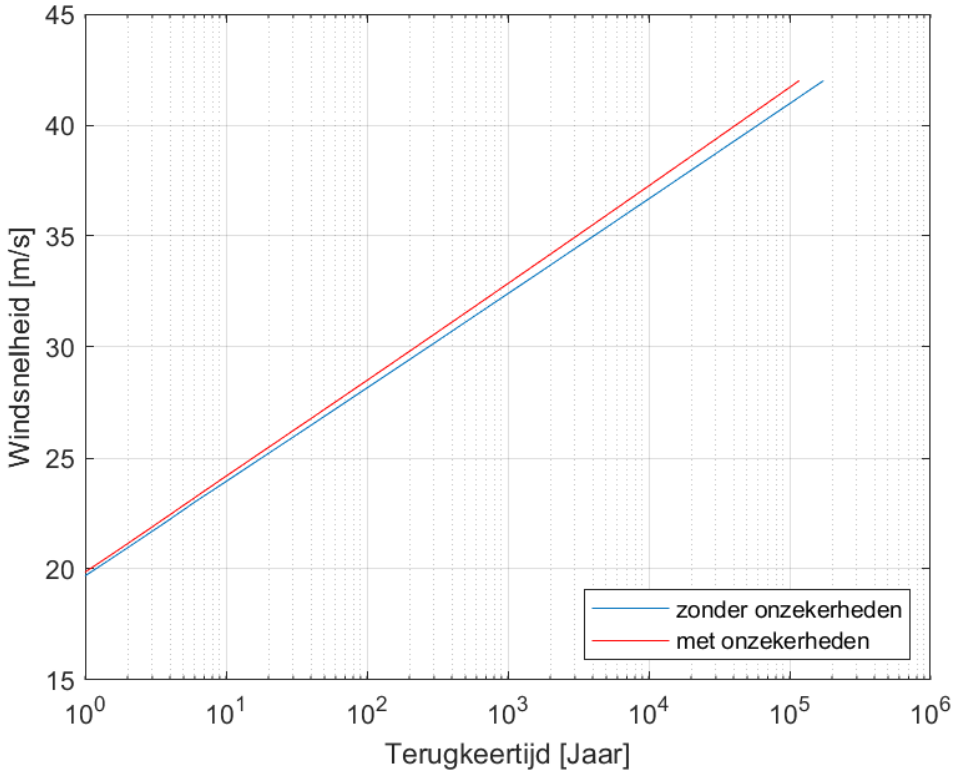

Figure A-1 Probability of exceedance curve for the wind speed at Vlissingen; blue line is without statistical uncertainties.

A.2 Extreme water level

At Vlissingen also water levels are being measured since 1881. The time series until 1985 has been used to determine the extreme value distribution of the water level conditioned on wind direction (Dillingh et al., 1993). These distributions have been corrected for the effect of sea level rise up till now. This correction is approximately 10 cm. The omnidirectional distribution has been determined and presented in Figure A-2. The 1/10.000 year value is 5.5 m + NAP.

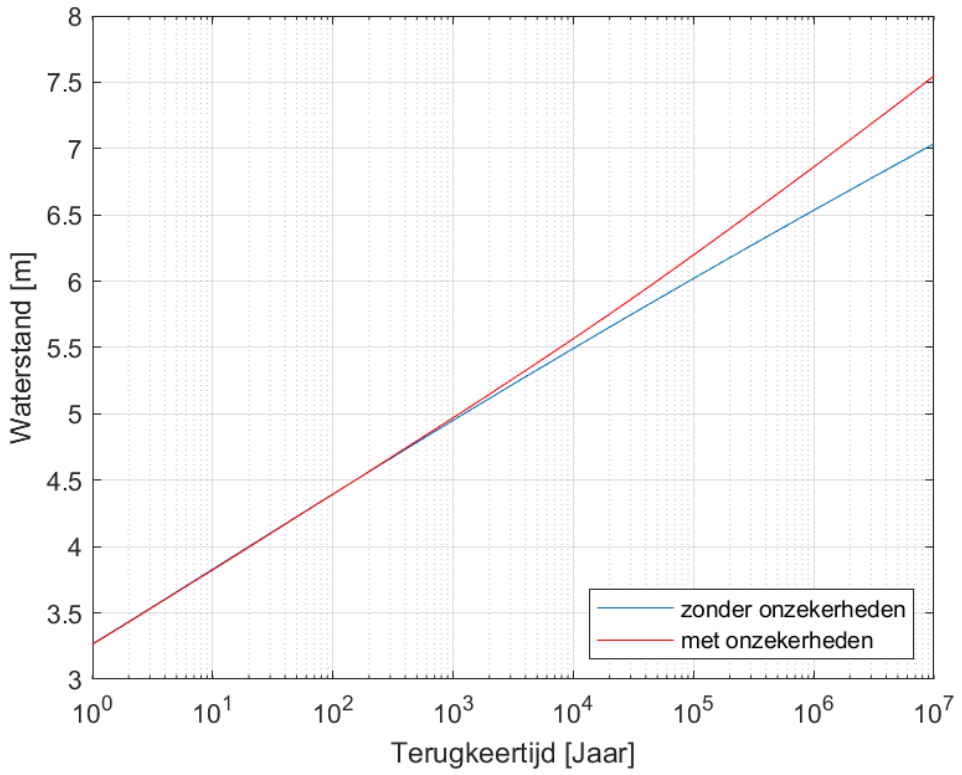

Figure A-2 Probability of exceedance curve of the water level at Vlissingen, with and without the statistical uncertainty integrated.

A.3 Extreme wave height

Whereas the extreme value distribution for wind and water level have been determined from measurements and form input for Hydra-NL, the extreme value distribution for wave height is the result of the combination of these variables needs to be determined with Hydra-NL. Within the Hydra-NL database there are six output points close to Borssele, shown in Figure A-3. At these locations the probability of exceedance has been determined and presented in Figure A-4. Clearly the variability between locations is significant. The 1/10.000 year value varies from 1.5 to 3.3 meters. This is due to the strong variation in bed height, as can be seen in Figure A-3.

When a more precise site location is determined (and potentially even changes in the bed height in the surrounding Western Scheldt), a more detailed assessment can be made regarding the occurrence of a significant wave height at the site location.

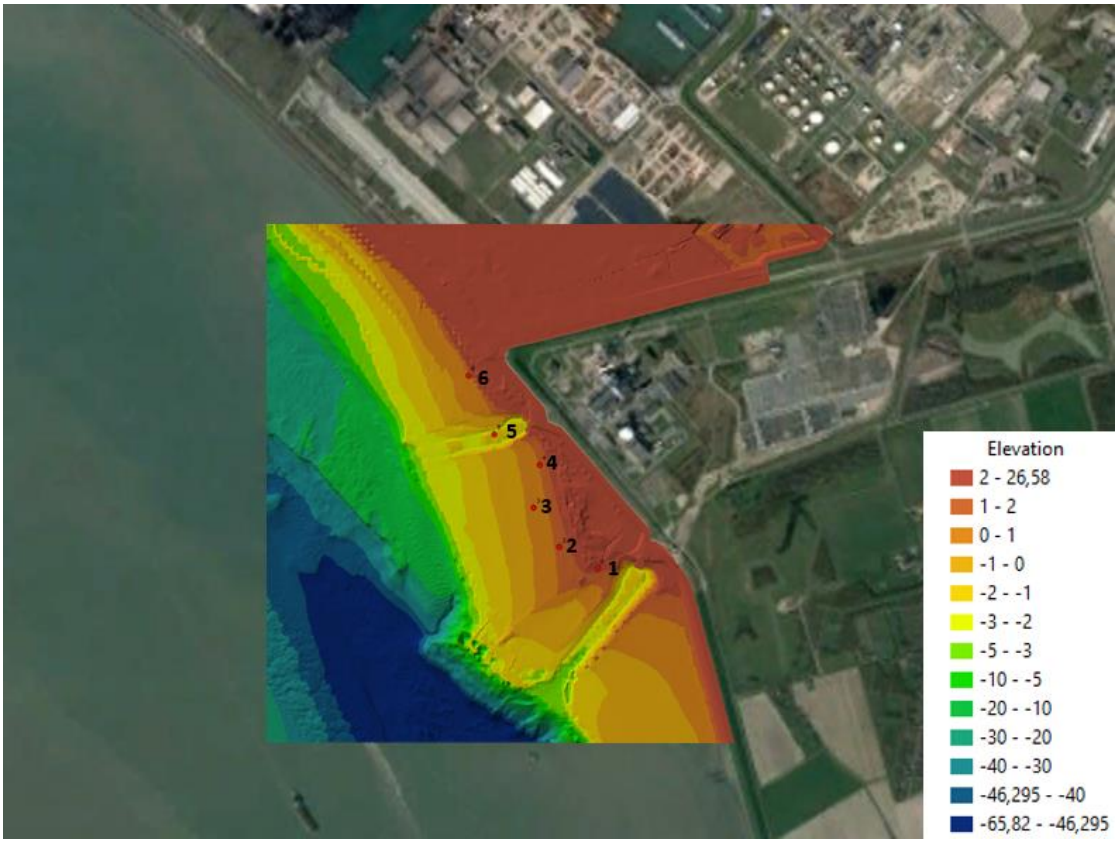

Figure A-3 Bed level and the six Hydra-NL close to Borssele.

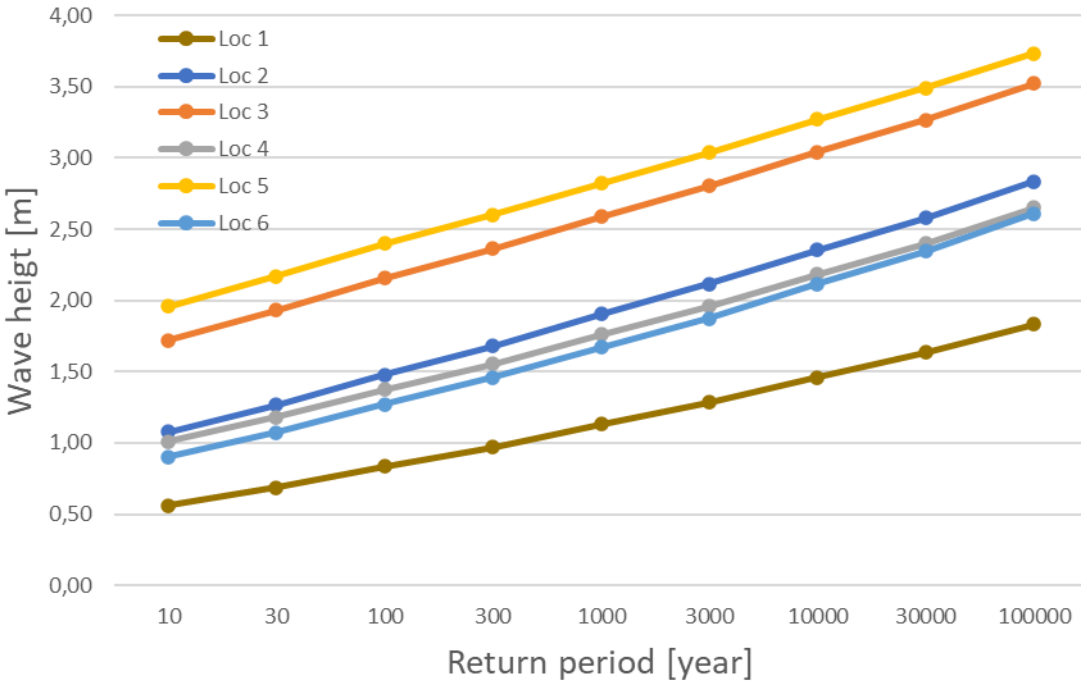

Figure A-4 Probability of exceedance curve for the wave height at six locations near Borssele.

A.4 Literature references

Caires (2009). Extreme wind statistics for the Hydraulic Boundary Conditions for the Dutch primary water defences SBW-Belastingen: Phase 2 of subproject "Wind Modelling". Deltares report 1200264-005, September 2009.

Dillingh, D.,de Haan, L., Helmers, R., Können, G.P. en van Malde J., 1993. De basispeilen langs de Nederlandse kust; statistisch onderzoek, Rijkswaterstaat, Dienst Getijdenwateren /RIKZ, Report DGW-93,023.

B Post-tropical cyclones and extreme precipitation in the Netherlands

By: Peter Siegmund (KNMI)
Date: June 7th, 2023

B.1 Introduction

This note provides a concise overview of current literature on several types of extreme weather in the present and future climate of the Netherlands. The focus is on post-tropical cyclones and on extreme precipitation. In addition, some information on hail, snow, and thunderstorms is provided.

B.2 Post-tropical cyclones in the Netherlands

B.2.1 Tropical and post-tropical cyclones

Tropical cyclones, or hurricanes, are extremely powerful storms that can develop over areas with warm sea water (> 26.5°C). Their energy source is the heat stored in seawater. By means of surface evaporation and subsequent condensation of the water vapor in the atmosphere by deep vertical motions, the heat of seawater is transferred to the atmosphere and finally converted into kinetic energy of tropical cyclones. The condensation leads to large amounts of rain fall.

Some tropical cyclones move northward along the US East Coast, losing their tropical character and turning into an extra-tropical storm. At the height of Newfoundland these post-tropical cyclones are carried by the jet stream towards Europe, and on the way they can regain strength under favorable conditions.

In a warming climate three different mechanisms might contribute to more and more intense post-tropical cyclones in Europe (Haarsma, 2021): 1) The strength of tropical cyclones is expected to increase. Stronger tropical cyclones will have a larger chance to survive over the cooler midlatitude sea water before entering Europe. 2) areas with high water temperatures are moving closer to Europe. 3) In the present climate, the north-eastern part of the tropical Atlantic is too cool for the genesis of tropical cyclones, but will become warmer than 26.5°C in a warmer climate. Tropical cyclones that originate in the middle and western part of the tropical Atlantic, usually follow a C-shape curve along the US east coast before entering Europe. On the contrary tropical cyclones that originate in the north-eastern part of the tropical Atlantic can, by traveling in north-easterly direction, take a short cut to Europe.

B.2.2 Observations

During the hurricane season (June-November) almost 9% of all severe storms in the North Sea (> 25 m/s) are originally hurricanes (Sainsbury et al., 2020). The average strength of these post-tropical cyclones is also larger than that of other storms. A study on European cyclones with tropical origin in reanalysis data revealed that in the period 1979-2013 53 hurricanes have entered the European area (Dekker 2018; KNMI, 2019). A very few of them still had hurricane strength when they hit the western part of the British Isles. The Netherlands has never been hit by a post-tropical cyclone with hurricane force (Beaufort 12; > 36 m/s). From the observational data the conclusion is therefore that the risk of the Netherlands being hit by a post-tropical cyclone with Beaufort 12 is negligible.

Europe was hit in October 2017 by hurricane Ophelia (Rantanen et al., 2020) that originated as the most northern eastward major (category 3) hurricane close to the Azores since the start of the observations and traveled in a straight line toward Ireland. It arrived there, after

reintensification, as a category 1 hurricane. It was partly caused by the locally very warm sea water temperatures (KNMI, 2019). Ophelia can be considered as a show case for what might become more common in a warmer climate (Haarsma, 2021). The British Isles are not necessarily a barrier: according to a model simulation, Ophelia could just as well have squeezed through the Straits of Calais to reach with hurricane force winds the Dutch coast (De Vries et al., 2018). The path of Ophelia was caused by the large-scale atmospheric circulation, and a slightly more easterly path is considered as a realistic possibility.

B.2.3 Future climate

In a warmer climate the strength of hurricanes is expected to increase (Knutson et al., 2020). Haarsma et al. (2013) used a very high resolution global climate model (~25 km grid size) with prescribed sea surface temperatures to show that greenhouse warming enhances the occurrence of hurricane-force (> 32.6 m/s) storms over western Europe during early autumn (August–October), the majority of which originate as a tropical cyclone. Summed over Norway, the North Sea, and the Gulf of Biscay the number of hurricane force storms increases from 2 to 13 over the 21st century. Over the North Sea the season of highest occurrence of storms (Beaufort 11-12, > 28.4 m/s) shifts from winter to autumn. In a more detailed analysis with the same model and resolution, Baatsen et al. (2015) found for a moderate warming scenario (RCP4.5) a major increase in the number of Autumn storms (Beaufort 11-12) originating in the tropical Atlantic: from 15 in the present (2002-2006) to 23 in the near future (2030-2034) and 37 in future (2094-2098) climate simulation (Figure B-1).

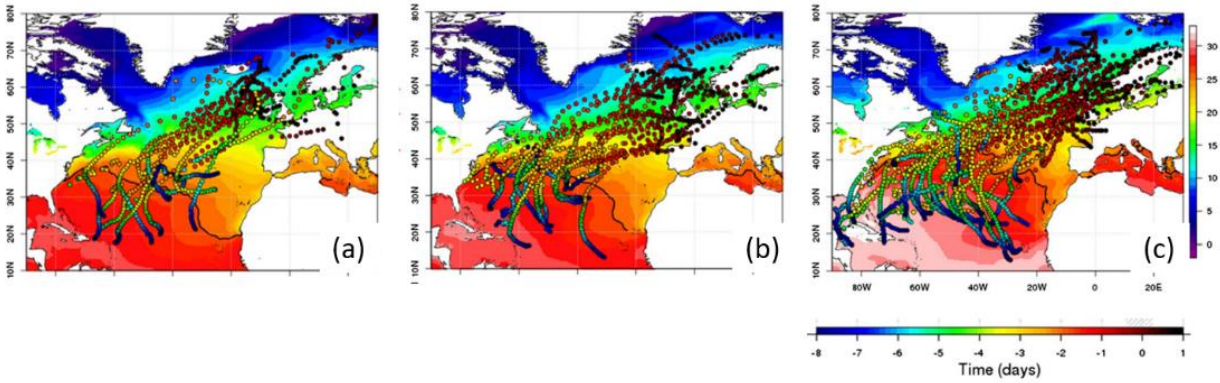

Figure B-1 Tracks for present (a), near future (b) and future (c) cyclones. The panels show the storm tracks and August-October mean sea surface temperatures (°C) for the respective periods, the thick black line is the 26 °C isotherm. The color scale of the circles indicates the duration in days before the moment that 11 Beaufort wind speed was reached. Source and more details: Baatsen et al., 2015.

Each simulation consists of a 6-member ensemble spanning 5 years, resulting in a 30 year dataset. The model simulated a wind speed for the North Sea of 37 m/s during a 30-year simulation that according to extreme value statistics would occur only once in the 20.000 year for the present climate (KNMI, 2019). Analysis of a simulation with another climate model, that of the Geophysical Fluid Dynamics Laboratory, has confirmed the increased risk of Western Europe to be hit by extra-tropical storm that origin from hurricanes (Liu et al. 2017). Further research with high-resolution climate models is required to further investigate the potentially high windstorm risk for Europe in the future of remnants of tropical cyclones (Haarsma, 2021).

Baatsen et al. (2015) also analyzed the dynamics of hurricanes that reach Europe. The mechanism for their intensification is the combination of the release of latent heat caused by heavy precipitation, which is the thriving force of hurricanes, and baroclinic instability, which is the mechanism for traditional mid-latitude storms. On their way to Europe the hurricanes transform into extra-tropical storms and expand in size. After an initial weakening during this

transformation when they enter the cooler waters of the Atlantic Ocean, they re-intensify in a later stage and regain hurricane force on entering the European coast. The storms of tropical origin also led to so-called atmospheric rivers with a large amount of water vapor, that will influence the future European climate accompanied by a higher potential for floods.

B.3 Extreme precipitation

B.3.1 Observations

Information of (extreme) rain in the Netherlands is provided by STOWA (2019) as the amount of rain at a given rainfall duration (two hours to eight days), which is exceeded with a certain frequency (twice a year to once a 1000 years) (Figure B-2). The information applies to any location in the Netherlands. For example, 50 mm rain in two days occurs on average once per 2 years, and 100 mm in two days once per 50 years. A heavy shower, defined by KNMI as 25 mm or more in one hour, occurs about once per 5 years.

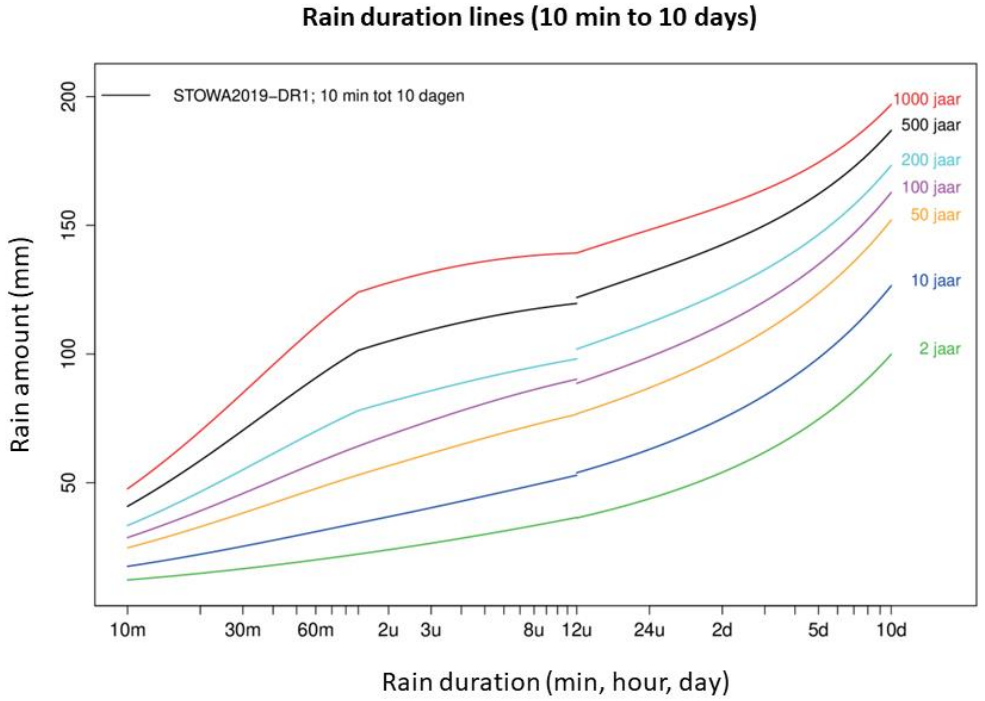

Figure B-2 Rain duration lines based on precipitation observations in the Netherlands for the whole year. Source: STOWA (2019).

The average amount of precipitation per year in the Netherlands increased by 9% between 1961-1990 and 1991-2020. If for each 30-year period the daily precipitations are ranked from highest to the lowest amount, for almost all ranked days the precipitation increase is also about 9%, except for the extremely wet days, for which the increase is up to 15% (KNMI, 2022). The number of very wet days – with at least 10 mm of precipitation in winter and at least 20 mm in summer – increased between 1961-1990 and 1991-2020 by about a quarter: from 4.3 to 5.3 days per winter and from 1.5 to 1.9 days per summer (KNMI, 2021). Between these periods the annual maximum precipitation per day in the Netherlands increased from 33 to 37 mm, and in De Bilt the annual maximum precipitation per hour increased from 15 to 19 mm.

B.3.2 Future climate

In a warmer climate, the atmosphere contains more water vapor. As a result, more precipitation falls from a shower. More water vapor in the atmosphere also means that more

heat of condensation is released, so that the air in showers rises faster and rains out faster. On the other hand, due to the condensation the air at higher altitudes warms more than air near the Earth's surface. This makes the atmosphere more stable, which slows down the vertical motions in the showers. The increase in condensation heat will probably have a greater effect and, therefore, extreme showers are expected to occur more often in the future.

In the KNMI'14 climate scenario's precipitation extremes increase throughout the year, even in the scenario's with an overall drying in summer. Such precipitation extremes can be caused by two meteorological phenomena: fronts associated with depressions, or rain showers caused by vertical instability of the atmosphere. Fronts are typical in winter, whereas showers are typical in summer, but often a combination of both occurs. While fronts are well resolved in the climate models used for developing the scenarios, rain showers, which cause the extreme precipitation peaks in summer, are not. Consequently, the change in precipitation extremes for a particular summer scenario is quite uncertain. In the KNMI'14 scenario's in winter the 10-day amount exceeded once in 10 years increases, relative to the refence period 1981-2010, by 6-17% around 2050 and 8-25% around 2085. In summer the daily amount exceeded once in 10 years increases by 2-22% around 2050 and 3-40% around 2085. The maximum hourly amount per year increases by 6-25% around 2050 and 8-45% by 2085.
In October 2023 the KNMI'23 climate scenario's will be published. First results indicate that the increase in moderate extreme hourly precipitation will be less than that in the KNMI'14 scenario's, and the increase in the highest extremes (above 50 mm per hour) will be about the same as that in the KNMI'14-scenarios (KNMI, 2021). New in the KNMI'23 scenario's compared to the KNMI'14 scenario's is that changes in rare, very extreme precipitation have been calculated with recurrence times of up to 1000 years.

B.4 Hail, snow, and thunderstorms

B.4.1 Hail

Due to the lack of long, high-quality measurements, little is known about possible trends in the frequency and intensity of hail. Information about hail in the future is only very limited. Because there is more water vapor in the atmosphere and vertical motions intensify, the largest hail stones are likely to become even larger. Regional climate models have been used to determine the frequency of hail with a diameter of 50 mm or more for Europe (Rädler et al., 2019). In the Netherlands, the frequency is highest in the southeast, about once every 15 years. At the end of this century, this frequency will increase, in case of an average global warming of 2 degrees, to about once every 10 to 12 years.

B.4.2 Snow

The number of days with snowfall in the Netherlands increases from the south-west to the north-east, from about 14 days per year in Zeeland (average for 2003-2020) to 24 days in the north-east. The KNMI'14 scenario's do not provide information for snowfall in the future, but given the future warming of the Netherlands the frequency of snowfall is expected to decrease. As a relative proxy for the frequency of snowfall one might use the frequency of frost days, on which the minimum temperature is below 0°C. Around 2050 the frequency of frost days is expected to be decreased by 30% to 60% relative to the reference period 1981-2010 (KNMI, 2015).

B.4.3 Thunderstorms

Thunderstorms are implicitly discussed in the section on extreme precipitation. Wind gusts and downburst that accompany thunderstorms can become stronger in the future (KNMI'21). Future changes in the frequency of lightning are uncertain.

B.5 References

Baatsen et al., 2015: Severe Autumn storms in future Western Europe with a warmer Atlantic Ocean, Clim Dyn 45:949–964. http://doi.org/10.1007/s00382-014-2329-8.

CLO, 2019: Neerslagextremen in Nederland, 1910-2019. Neerslagextremen in Nederland, 1910-2019 | Compendium voor de Leefomgeving (clo.nl).

Dekker et al., 2018: Characteristics and development of European cyclones with tropical origin in reanalysis data, Clim Dyn 50:445–455. https://doi.org/10.1007/s00382-017-3619-8.

De Vries et al., 2018: Als orkaan Ophelia Nederland had bereikt. Meteorologica, 27, 4-8. https://www.nvbm.nl/meteorologica/archief/2010-2019/2018/september-2018.

Haarsma et al., 2013: More hurricanes to hit Western Europe due to global warming. Geophys. Res. Let., 40, 1783-1788. https://doi.org/10.1002/grl.50360.

Haarsma, R., 2021: European Windstorm Risk of Post-Tropical Cyclones and the Impact of Climate Change, Geophys. Res. Let., 48. https://doi.org/10.1029/2020GL091483.

KNMI, 2015: KNMI'14 climate scenarios for the Netherlands; A guide for professionals in climate adaptation, KNMI, De Bilt, The Netherlands, 34 pp. https://cdn.knmi.nl/system/data_center_publications/files/000/070/807/original/Brochure_KNMI14_EN_2015.pdf?1653079346 .

KNMI, 2019: Climatology of the PALLAS site near Petten (not publicly available).

KNMI, 2021: KNMI Klimaatsignaal'21: hoe het klimaat in Nederland snel verandert, KNMI, De Bilt, 72 pp. https://cdn.knmi.nl/knmi/asc/klimaatsignaal21/KNMI_Klimaatsignaal21.pdf .

KNMI, 2022: Als het regent, valt er 9% meer regen dan 50 jaar geleden, KNMI klimaatbericht, https://www.knmi.nl/over-het-knmi/nieuws/als-het-regent-valt-er-9-meer-regen-dan-50-jaar-geleden .

Knutson et al., 2020: Tropical Cyclones and Climate Change Assessment: Part II: Projected Response to Anthropogenic Warming. BAMS. 101, E303-E322. https://doi.org/10.1175/BAMS-D-18-0194.1 .

Liu et al., 2017: The present-day simulation and twenty-first-century projection of the climatology of extratropical transition in the North Atlantic. J. Clim., 30(8), 2739-2756. https://doi.org/10.1175/JCLI-D-16-0352.1 .

Rädler et al., 2019: Frequency of severe thunderstorms across Europe expected to increase in the 21st century due to rising instability. npj Clim Atmos Sci 2, 30. https://doi.org/10.1038/s41612-019-0083-7 .

Rantanen et al., 2020: The extratropical transition of Hurricane Ophelia (2017) as diagnosed with a generalized omega equation and vorticity equation. Tellus, Series A: Dynamic Meteorology and Oceanography, 72(1), 1–26. https://doi.org/10.1080/16000870.2020.1721215 .

Sainsbury et al., 2020: How important are post-tropical cy1clones for European windstorm risk? Geophysical Research Letters, 47, e2020GL089853. https://doi.org/10.1029/2020GL089853 .

STOWA, 2019: Neerslagstatistiek en -reeksen voor het waterbeheer 2019, STOWA2019-19. STOWA 2019-19 neerslagstatistieken.pdf and STOWA 2019-19A brochure neerslagstatistieken.pdf.

C Tsunami risks at Borssele site

By: Reimer de Graaff
Date: July 17, 2023

C.1 Introduction

Tsunamis are waves propagating in the sea as a result of a sudden vertical displacement of the water column due to, for example, a submarine earthquake or landslide. Offshore, tsunamis can have wavelengths of up to a few 100 km's and wave amplitudes of usually less than 1 m. When tsunami waves approach the coast, the propagation speed decreases and the amplitude increases, potentially leading to coastal inundation.

The occurrence of destructive tsunamis in the North Sea and along the Dutch coast is very unlikely since there are no major tsunami sources (esp. earthquakes or landslides) present in the North Sea. Moreover, the shallow waters of the North Sea cause strong dissipation of a tsunami coming from the Atlantic Ocean or Norwegian Sea, which will therefore lose most of its energy before reaching the Dutch coast (e.g. DEFRA, 2005, Chacón-Barrantes et al., 2013, Bork et al., 2007). In absence of detailed studies on tsunami risks for the Borssele site, this section summarizes the probability of tsunami occurrence and estimated maximum tsunami wave heights at the Dutch coast and specifically Borssele, based on a literature review combined with expert judgement.

C.2 Potential sources for tsunami's reaching Borssele site

Potential sources of tsunamis reaching the Dutch coast are submarine earthquakes at (distant) subduction zones or at (local) fault zones, submarine landslides, erupting or collapsing volcanoes, meteorites, or fast-propagating storm fronts along the coast causing meteo-tsunamis. Each of these potential sources are discussed briefly below.

C.2.1 Tsunamis due to submarine earthquakes at (remote) subduction zones

Most tsunamis in the world are caused by sudden vertical motions in the earth's crust at so-called subduction zones, where one tectonic plate dips under another tectonic plate with lower density. These subduction zones, and therefore the origin of tsunamis, are mostly located in the Pacific Ocean ('Ring of Fire', see Figure C-1).

Subduction zones in the Atlantic Ocean are less extensive and more passive than the ones in the Pacific Ocean. The only known significant tsunami that occurred in the Atlantic Ocean due to plate tectonics was in 1755 AD. This tsunami was the result of M_w 8.5 submarine earthquake with its epicenter with about 200 km to the west of Portugal (Sousa et al., 1992). According to historic evidence published in DEFRA (2005) it is unlikely that the Lisbon 1755 tsunami has led to a significant tsunami at the Dutch coast. There is a chance that tsunamis will be triggered at the same subduction zone in the future. However, it is expected that these will be less severe than in 1755 AD (Baptista et al., 2003).

The same accounts for a tsunami generated due to a submarine earthquake in the Caribbean. According to DEFRA (2005) it is likely that an extreme submarine earthquake event at the Caribbean subduction zone has already happened, but that this event did not lead to a significant tsunami reaching the coasts of northwestern Europe.

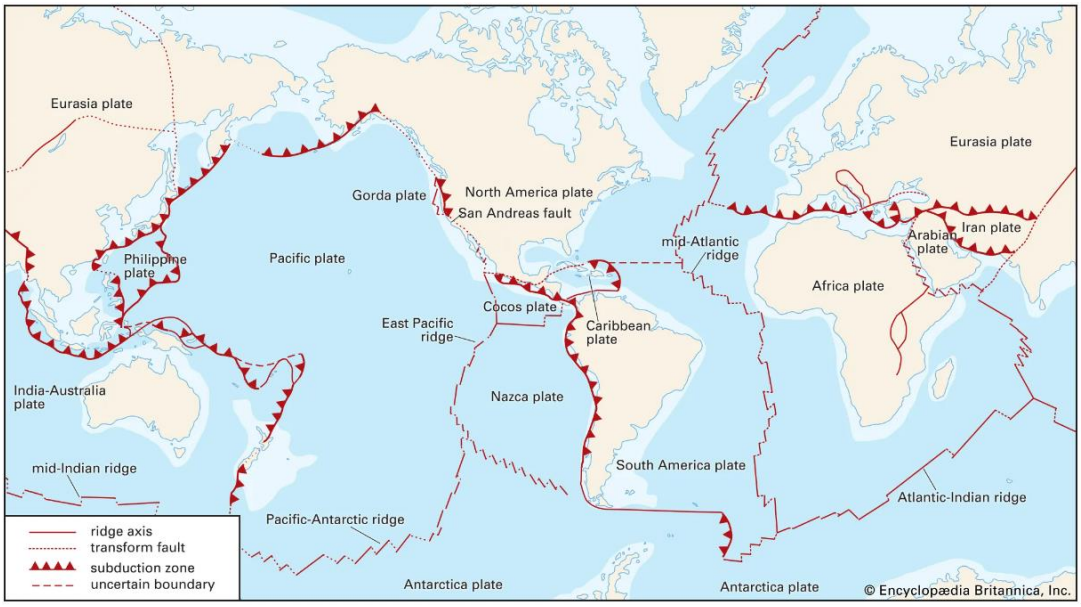

Figure C-1 Subductions zones in the world (figure source: https://www.britannica.com/science/subduction-zone).

C.2.2 Tsunamis due to submarine earthquakes at fault zones in the Southern North Sea

In DEFRA (2005) it is stated that the occurrence of a 6.5 M_w earthquake in the North Sea, which is within the lower range for tsunamigenic earthquakes, cannot be ruled-out. In the North Sea, a few submarine earthquakes have been observed in the past, namely a 5.7 M_w earthquake in 1927 with its epicenter in the northern part of the North Sea (Viking Graben) and a 6.1 M_w earthquake in 1931 with its epicenter in the southern part of the North Sea (Sole Pit Basin or Dogger Bank). According to DEFRA (2005) there is no evidence of significant tsunami waves reaching the UK or Dutch coasts as a result of these two earthquakes.

C.2.3 Tsunamis due to submarine landslides

After submarine earthquakes, submarine landslides are the second most frequent tsunami source worldwide. Submarine landslides are however much more diverse in nature and very difficult to predict (Løvholt et al., 2020). Near their source, landslide-generated tsunamis may result in higher tsunami wave heights than seismically generated tsunamis, but will usually lose energy quickly due to wave energy dissipation and/or divergence, and rarely affect distant coasts (NOAA, 2023).

For the Dutch coast the most likely source of a landslide tsunami is off the coast of Norway (Figure C-2). Here, the so-called Storegga Slide occurred about 8200 years ago, which is believed to have generated a large tsunami in the northern part of the North Sea according to sediment deposits along the coasts of Norway, Faeroes Islands, Shetland Islands and in the area of the Dogger Bank (Bondevik et al., 2005; Gaffney et al., 2020). When this tsunami wave propagated into the central and southern part of the North Sea, it is likely to have reached the Dutch coast (e.g. Twigt and Blaas, 2007). Other landslides may occur in the same area, but probably with smaller volumes as compared to the Storegga Slide (DEFRA, 2005) and therefore with much smaller expected typical tsunami wave heights.

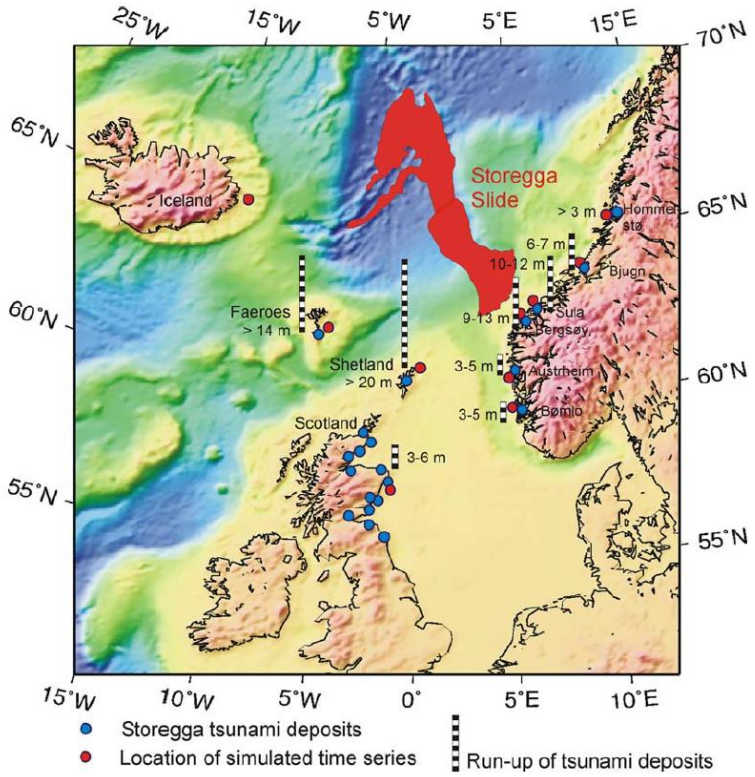

Figure C-2 Map of the Storegga Slide, run-up heights (bars) and study locations (dots) from Bondevik et al., 2005.

C.2.4 Tsunamis due to erupting or collapsing volcanoes

Ocean-based volcanoes that erupt or collapse are a potential trigger for tsunamis. It has been suggested by Ward and Day (2001) that a landslide on the flank of La Palma, one of the Canary Islands, will result in a potentially very high tsunami in the North Atlantic Ocean. Nevertheless, numerical model simulations by Abadie et al. (2020) show that a tsunami originating from La Palma will not be able to propagate into the North Sea (Figure C-3). Other potential sources of volcanogenic tsunamis are Cape Verde or along the Mid-Atlantic Ridge, however, it is very unlikely that such events will result in significant tsunami wave heights at the North Sea coasts (DEFRA 2005).

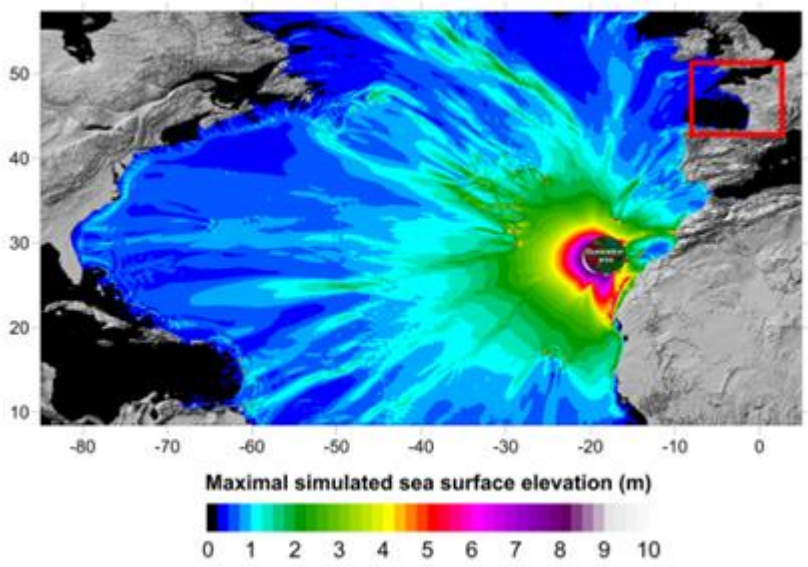

Figure C-3 Maximum wave height as a result of a hypothetical tsunami due to flank collapse at La Palma (from: Abadie et al., 2020).

C.2.5 Tsunamis due to meteorite impacts

The chance of a significant tsunami resulting from a meteorite striking the Atlantic Ocean or bordering seas is extremely low. Paine (1999) argues that only meteorites with a diameter of 200 m or more will trigger tsunamis. According to the diagram in Figure C-4 the chance of a 200 m wide meteorite hitting the earth has a recurrence interval of at least 10.000 years, obviously with a very large degree of uncertainty. The chance of such a meteorite hitting the North Atlantic Ocean and resulting in a tsunami that will affect the Dutch coast, will be even lower.

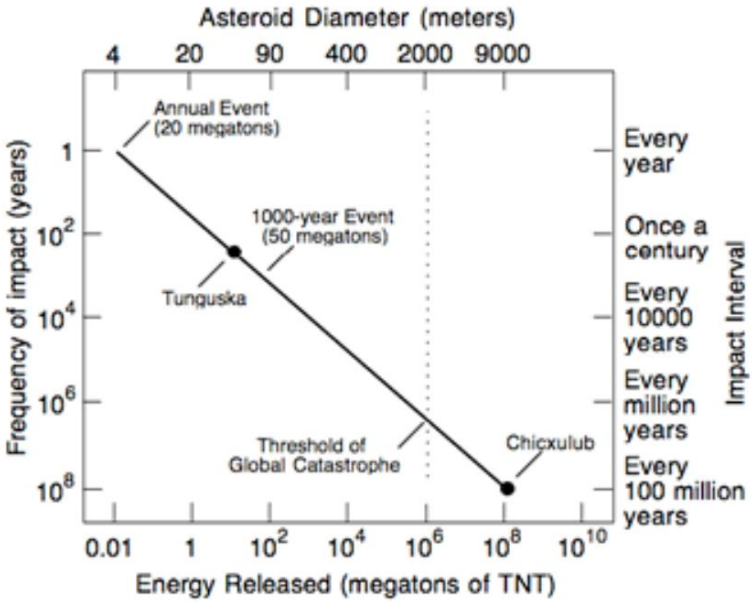

Figure C-4 Relationship between the size of a meteorite and the frequency of occurrence (from: geology.com/articles/near-earth-asteroids.shtml)

C.2.6 Tsunamis due to fast moving storm fronts

Fast moving convective storm fronts, leading to rapid changes of surface pressure, can result in long waves propagating along the coast (De Jong, 2004). These meteo-induced long waves are referred to as seiches (refer to Appendix D) or meteotsunamis.

Meteotsunamis are probably the most likely source of tsunamis at the Dutch coast. The most recent meteotsunami at the Dutch coast occurred on May 29, 2017 (Figure C-5), with a measured 0.9 m wave height along the coast and an estimated wave run-up height of 2 m on the beach (Sibley et al., 2021). In Frère et al. (2014) a meteotsunami in 2011 is presented, propagating from the south of Portugal, along the French coast and into the English Channel. According to the Royal Dutch Meteorological Institute (KNMI), meteotsunamis occur several times per year but are often unnoticed[4]. Another significant meteotsunami affecting the Dutch Coast (and Lake IJssel) occurred on July 11th, 1984. According to KNMI, the intensity of meteotsunamis may increase due to climate change.

[4] https://www.knmi.nl/kennis-en-datacentrum/achtergrond/meteo-tsunami-treft-nederlandse-kust)

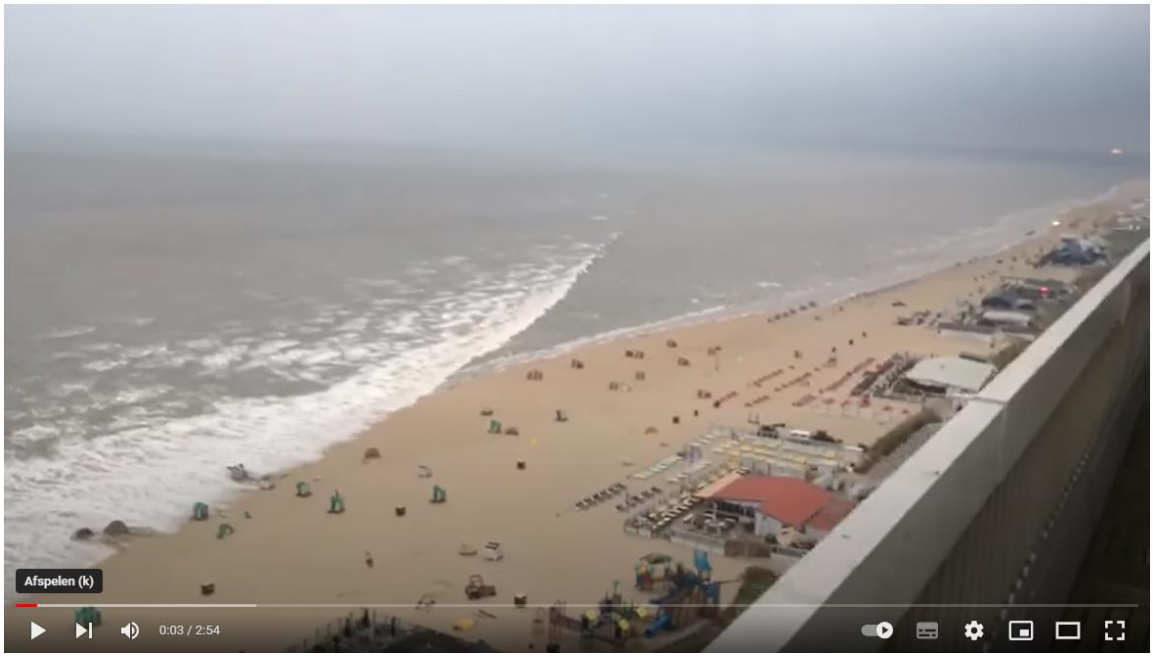

Figure C-5 Video still from the meteotsunami at the Dutch coast on May 29, 2017 (source: https://www.youtube.com/watch?v=CjQk_xt_WU0).

C.2.7 Estimates of maximum tsunami height and recurrence intervals

As mentioned in the introduction of this section, tsunami wave heights in the southern part of the North Sea are limited which is partly related to the shallow water depths and resulting energy dissipation. Bork et al. (2007) illustrated this effect by making simulations with realistic water depths (up to approximately 200 m) in the North Sea and assuming a fictional deep water of 500m in a separate calculation. The left panel of Figure C-6 shows that the tsunami wave heights reaching the North Sea are limited when considering realistic water depths. The right panel of that figure shows that if the North Sea would have been much deeper (500 m in this case, although the precise value is not critical for making this point), much higher tsunami wave heights would occur in this area. However, this will not be the case in reality.

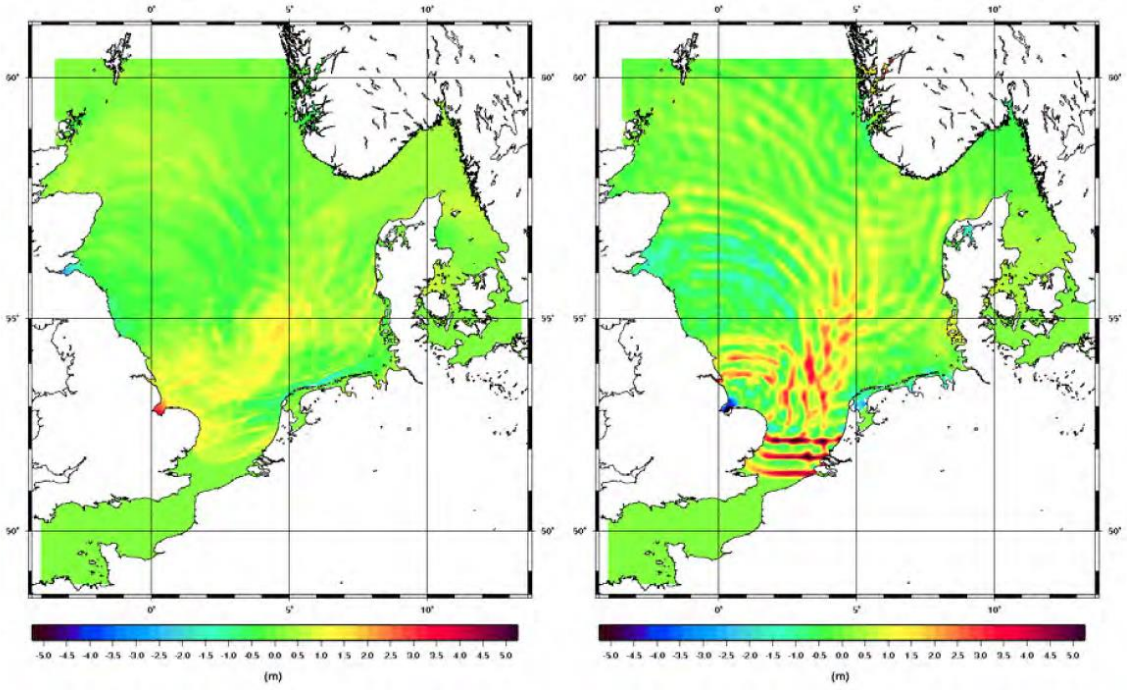

Figure C-6 Results of tsunami model simulations in the North Sea assuming realistic water depths (left) and uniform deep water of 500m (right) (from: Bork et al., 2007)

Similar to tsunami waves approaching the Dutch coast from the north, tsunami waves propagating through the British Channel will also be largely attenuated due to the limited width and depths of the channel (e.g. Chacón-Barrantes et al., 2013).

On the basis of the literature review combined with expert judgement, the table below summarizes indicative values of the maximum possible tsunami wave heights along the Dutch coast, and their estimated probability of occurrence for the various tsunami sources.

Table C-1 Maximum possible tsunami wave heights at the Dutch coast, and its estimated probability of occurrence for various tsunami sources.

Tsunami source	Indications of upper estimates of tsunami wave heights along the Dutch Coast	Very rough indication of probability of associated return periods [years]	Literature reference
Submarine earthquakes at subduction zones	insignificant	Not relevant	DEFRA, 2005
Submarine earthquakes at fault zones in the North Sea	2 m 0.75 m 0.50 m	100.000 5.000 500	Van Malde, 1990 Bijl, 1993
Submarine landslides	1.5 m	100.000	Chacón-Barrantes et al., 2013
Erupting or collapsing volcanoes	insignificant	beyond practical (design) relevance	Abadie et al., 2020
Meteorite impacts	Unknown	Very unlikely	Paine, 1999
Fast moving storm fronts	1 m	10 - 50	Sibley et al., 2021

No information was found in literature on the propagation of tsunami waves from the southern part of the North Sea into the Western Scheldt. However, it is expected that the tsunami wave height will dissipate while propagating into the Western Scheldt, in a similar way as seiches (refer to Section ZZZ).

C.3 Conclusions

The literature study on tsunamis potentially affecting the Dutch coast showed that either a landslide in the northern part of the North Sea or a local earthquake-generated tsunami in the southern part of the North Sea can result in maximum wave heights of between 1.5 – 2 m. The probability of occurrence of such events are however very low (about once in 100.000 years). Other tsunamigenic sources, such as from earthquakes at remote subduction zones, volcanoes or meteorites, are not expected to result in significant tsunami wave heights at the Dutch coast. The most probable cause of tsunami wave heights of up to 1m are from fast moving storm fronts (meteotsunamis or seiches). It is expected that tsunami wave heights will be lower at Borssele site compared to the values reported in this section for along the Dutch coast, however, no information is yet available to confirm this.

C.4 Literature references

Abadie et al., 2020. La Palma landslide tsunami: calibrated wave source and assessment of impact on French territories. Nat. Hazards Earth Syst. Sci., 20.

Baptista, M.A., Miranda, J.M., Chierici, F. and Zitellini, N., 2003. New study of the 1755 earthquake source based on multi-channel seismic survey data and tsunami modelling. Natural Hazards and Earth System Sciences, 3: 333-340.

Bijl, 1993. Tsunami golven in het Noordzee gebied. Master Thesis. Technische Universiteit Delft.

Bondevik et al., 2005. The Storegga Slide tsunami-comparing field observations with numerical simulations, Marine and Petroleum. Geology 22.

Bork et al., 2007. Tsunami - a study regarding the North Sea coast. Berichte des Bundesamtes für Seeschifffahrt und Hydrographie Nr. 41/2007.
Chacón-Barrantes et al., 2013. Several tsunami scenarios at the North Sea and their consequences at the German Bught. Science of tsunami hazards. ISSN 8755-6839. Journal of Tsunami Society International. Vol. 32, No. 1.

DEFRA, 2005. The threat posed by tsunami to the UK. British Geological Survey, UK Met Office, Proudman Oceanographic Laboratory, HR Wallingford.

De Jong, 2004. Origin and prediction of seiches in Rotterdam harbour basins. PhD Thesis, Delft University, Faculty of Civil Engineering and Geosciences. SBN 90-9017925-9.

Gaffney et al. 2020: https://www.mdpi.com/2076-3263/10/7/270.

Løvholt et al., 2020. On the landslide tsunami uncertainty and hazard. Landslides (2020) 17:2301–2315.DOI 10.1007/s10346-020-01429-z.

Van Malde, 1990. Onderzoek naar mogelijke beïnvloeding van Nederlandse getij-waterstanden door aardbevingen en naar historische “Moerzeeën”, Nota Rijkswaterstaat GWAO-90.009.

NOAA, 2023. https://www.noaa.gov/jetstream/tsunamis/tsunami-generation-landslides

Paine, 1999. Asteroid impacts: the extra hazard due to tsunami. Science of Tsunami Hazards, Vol 17, No. 3 (1999).

Sibley et al., 2021. Convective rear-flank downdraft as driver for meteotsunami along English Channel and North Sea coasts 28–29 May 2017. Natural Hazards 106(1-2):1-21. DOI: 10.1007/s11069-020-04328-7.

Sousa et al., 1992. Laboratorio Nacional de Engenharia Civil. Report 36/92-NDA, Lisbon.

Twigt and Blaas, 2007. Storegga tsunami simulations. R&D Coastal Flooding. Report Z3929. Delft Hydraulics.

Ward and Day, 2001. Cumbre Vieja Volcano -- Potential collapse and tsunami at La Palma, Canary Islands. American Geophysical Union. Paper number 2001GL000000.

D Estimate of amplitude of seiches at Borssele site

By: Julius Sumihar based on input by Martijn de Jong
Date: July 5th, 2023

D.1 Introduction

Seiches are standing, resonant long waves inside (semi-)enclosed basins. In the study of de Jong (2015a), Western Scheldt is considered as one of the areas where seiches can occur. Seiches in the Western Scheldt are typically caused by weather processes. Seiches can cause safety and operational issues at for example harbors, and they can add to the hydraulic loading on coastal structures and developments.

This section provides an estimate of seiche or long-wave amplitude at Borssele based on literature review and expert assessments.

D.2 Physics of seiches

Potential seiche inducing long wave events on the North Sea, and the resulting seiche events inside the ports along the Dutch coast, are generated by passing low-pressure systems and cold fronts. Associated wave periods fall within the range of a few minutes up to a few hours, so in between wind/swell waves and the tides. All such long-wave events coincide with a storm, although not all storms lead to seiche events (De Jong 2004). The correlation between seiche and incoming long waves is determined by the local geometry characteristics (primarily horizontal geometry dimensions and water depth). De Jong (2015c) shows for example that at Terneuzen, further upstream along the Western Scheldt, there is no correlation between the local net seiche effect and the surge level. This is different from the characteristic at Rotterdam harbor where a (slight) positive correlation was found between seiche and surge level (Reimerink and de Jong, 2014).

Typically, these long-wave events reaching the Dutch coastline are either short events (a couple of hours) or longer events (in the order of 24 hours). These durations are linked to two types of generating cold fronts (see e.g. De Jong et al., 2002, De Jong et al, 2003, De Jong, 2004) and correspond to generation of these long waves by a cold front combined with either squall-induced pulses or squall-induced oscillations. In case of a single squall-induced pulse a port geometry may respond with a seiche movement inside a basin that gradually reduces in height due to damping/energy loss.

D.3 Estimates of seiches magnitude

When enough representative and suitable water level measurements are available (i.e. at the required location, with a fitting sampling rate, sufficiently long duration), a procedure for analyzing the seiche statistics can be performed, as applied for Rotterdam, IJmuiden and Terneuzen (Reimerink and de Jong, 2014; de Jong et al, 2014; de Jong, et al, 2020). Without a suitable local water level measurement series specifically representative for Borssele, we rely on an estimate based on expertise documented in literature.

In the Western Scheldt, water level fluctuations can consist of local seiches and other long wave phenomena coming from the open sea. The occurrence of local seiches requires that a local water body is at least partially confined, which allows the formation of resonant standing waves. For the proposed Borssele site, at the time this report is prepared, the exact layout is unknown. For the moment it is assumed that the plant will be bordering directly onto the Western Scheldt. As this estuary is (for the purposes of seiches) an unconfined water body,

with resonant time scales way beyond those of the long waves coming in from the North Sea, local seiches will not occur . This means that in absence of a geometry the incoming long waves from the North Sea will reach and pass the site without (seiche-like) amplification. Therefore, the estimation of typical local long-wave amplitudes will focus here on long waves generated by the squall-induced pulses and oscillations at the open sea that propagate upstream the Scheldt estuary, following the study of de Jong (2015b).
First expert-based estimations of the occurrence frequency and typical amplitudes of long waves propagating from the North Sea into Western Scheldt can be found in the report of Delta Commission (RWS, 1961) and in the study by Hoek (1971).

The Delta Committee (RWS, 1961) reported that (responses to) squall-induced pulses are in general higher than the squall-induced oscillations. This distinction is relevant in case of a local geometry and a response that can be limited to a damped oscillation at an eigen-frequency (pulse forcing), or an amplified resonant response (longer duration event). This explains why the latter generally show the highest amplitude responses. At the open sea off the Western Scheldt, the amplitudes of the incoming long waves were estimated at 0.30 m. The Delta Committee described that the amplitudes decrease further into the estuary due to (shallow-water) damping effects (leaving around 0.05 m at a location 20 km upstream into the estuary).

Hoek (1971) made an inventory of squall-induced oscillations (long waves from the North Sea) along the Dutch coasts and how they propagate into the Western Scheldt. The study reported that the amplitude of the squall-induced oscillations in the open sea can reach 0.2-0.3 m. Hoek (1971) also concluded that the squall-induced oscillations can appear at any location along the Dutch coasts and that local (port) geometry characteristics play an important role in determining the effect and potential impacts of such long waves. Hoek (1971) suggested that at Western Scheldt, squall-induced oscillations can occur, but with smaller amplitudes further upstream into the estuary due to energy losses/damping, which is consistent with the Delta Commission report (RWS, 1961).

The two studies cited and summarized above have been used to estimate typical long-wave amplitudes at Terneuzen based on expert judgment (de Jong, 2015b). Based on these results, assuming no wave attenuation from the open sea[5], a conservative estimate of the amplitude of meteorologically generated long waves at Borssele is 0.30 m.

D.4 Conclusions

Based on literature review, the best estimate currently available of the long wave amplitude at Borssele site is 0.30 m. This amplitude refers to the long waves generated by the squall-induced pulses and oscillations at the open sea. No local effect of resonance is included, as it is unknown for now whether a local geometry will play a role in potential local resonant responses. For a more refined estimate, and even more so if a local geometry would play a role, analysis of water level measurements is required. Such water level measurements should preferably be available for a location at or close to Borssele, with a suitable data sampling rate, and for a long duration.

D.5 Literature references

De Jong, M.P.C., J. A. Battjes and L. Holthuijsen (2002), Generation of Seiches by Two Types of Cold Fronts, March 2002, DOI: 10.1061/40604(273)161 Conference: Fourth International Symposium on Ocean Wave Measurement and Analysis.

[5] With the location of Borssele quite close to the mouth of the Western Scheldt Estuary this is a fitting assumption.

De Jong, M.P.C., L. Holthuijsen and J.A. Battjes (2003), Generation of seiches by cold fronts over the southern North Sea, April 2003, Journal of Geophysical Research Atmospheres 108(4):3117, DOI: 10.1029/2002JC001422.

De Jong, M.P.C., 2004, Origin and prediction of seiches in Rotterdam harbour basins, Delft University of Technology, 2004, ISBN 90-9017925-9.

De Jong, M.P.C., S.P. Reijmerink and M.J.A. Borsboom, 2014, Statistiek seiches buitenhaven IJmuiden voor ontwerp nieuwe zeesluis, Rapport 1209945-000-HYE-0002.

De Jong, M., 2015a, Inventarisatie van seiches-locaties in Nederland – Verkenning en Plan van Aanpak, Tech. Rapport, Deltares, 1220039-010-VEB-0001.

De Jong, M., 2015b, Expert-interpretatie seiches buitenhavens Terneuzen, Deltares Memo, 1220093-003-GEO-0002.

De Jong, M., 2015c, Statistische analyse seiches buitenhavens Terneuzen, Deltares Memo, 1220093-003-GEO-0003.

De Jong, M.P.C., S.P. Reijmerink, and J.V.L. Beckers, 2020, Meteorologically generated long-period waves and their impact on the Dutch primary national flooding protection system, Natural Hazards, **106**, 1421–1443 (2021). https://doi.org/10.1007/s11069-020-04081-x.

Hoek, W.J.N., 1971, Onderzoek naar het vóórkomen van buioscillaties in de monding van de Westerscheide - Onderzoek naar de effecten van buioscillaties op een haven ontwerp, MSc thesis TUD.

Reijmerink, S.P. and M.P.C. de Jong, 2014, Actualisatie seiches Rotterdam WTI2017, Waterstandsafhankelijke seiche-waarden, Deltares Report, 1209433-006-HYE-0002.

RWS, 1961, Rapport Deltacommissie, Bijdragen III, Beschouwingen over stormvloeden en getijbeweging.

Deltares is an independent institute for applied research in the field of water and subsurface. Throughout the world, we work on smart solutions for people, environment and society.

Deltares

www.deltares.nl